DEVELOPMENT OF TIME DOMAIN BEHAVIOURAL NON-LINEAR MODELS FOR MICROWAVE DEVICES AND ICS FROM VECTORIAL LARGE-SIGNAL MEASUREMENTS AND SIMULATIONS

D. Schreurs, N. Tufillaro*, J. Wood**, D. Usikov*, L. Barford*, D.E. Root**

K.U.Leuven, Div. ESAT-TELEMIC, Kardinaal Mercierlaan 94, B-3001 Leuven, Belgium
E-mail: dominique.schreurs@esat.kuleuven.ac.be, Fax: +32-16-321986, Phone: +32-16-321821
*Agilent Laboratories, Palo Alto, CA 94304, USA
**Agilent Technologies Microwave Technology Center, Santa Rosa, CA 95403, USA

ABSTRACT

We have developed a procedure to determine a behavioural non-linear model for microwave devices and ICs that is directly based on vectorial large-signal measurements. For the examples of a HEMT and an amplifier IC, we represent the terminal currents in the time domain by a dynamic model that is fitted to the embedded terminal voltages.

INTRODUCTION

The recent availability of vectorial large-signal measurement setups, e.g., (1),(2), has made it possible to develop new non-linear modelling approaches that are no longer dependent on the small-signal approximation and hence S-parameter measurements. The modelling techniques proposed so far concern mainly gray-box model extractions (3),(4) and black-box model identifications in the frequency-domain (5). In this work, we have developed a black-box time domain modelling procedure, which means that the microwave device is described by a dynamical model. The approach is to find the functional relationship between the terminal currents, the terminal voltages and possibly also their higher order time derivatives, i.e., in case of a two-port device:

$$I_1(t) = f_1\left(V_1(t), V_2(t), \dot{V}_1(t), \dot{V}_2(t), \ddot{V}_1(t), \ldots, \dot{I}_1(t), \dot{I}_2(t), \ldots\right) \quad (1)$$

$$I_2(t) = f_2\left(V_1(t), V_2(t), \dot{V}_1(t), \dot{V}_2(t), \ddot{V}_1(t), \ldots, \dot{I}_1(t), \dot{I}_2(t), \ldots\right) \quad (2)$$

In the next section, we describe in detail the developed modelling procedure. The different steps are clarified by applying them to a microwave transistor, a HEMT, and a circuit, an IC amplifier. The final modelling results will be presented in the subsequent section.

MODELLING PROCEDURE

The proposed modelling method is based on time domain data of the DUT. These data can be obtained by either performing vectorial large-signal measurements or by simulating a transistor-level model of the DUT using harmonic-balance or a time-domain analysis. In the latter case, the purpose is to determine a lower-dimensional behavioural model of the DUT of which the validity will be limited to particular applications. An important decision at the start of the modelling process is indeed the definition of the operation region for which the model is to be developed, because the gathered time domain data need to cover this region well.
For the example of a HEMT, we first define a minimum and maximum gate-source (V_1) and drain-source voltage (V_2). V_1 typically ranges from V_T to V_{bi}, the turn-on of the Schottky diode, and V_2 ranges from 0 V to the usual V_{supply} for the considered technology. Next, we divide this area in a grid, which may be non-equidistant. The purpose of the data gathering process is to have a minimum number of time domain data, e.g., 10, in each of the boxes defined by the grid. The advantage of applying a large-signal excitation to the device instead of the (conventional) small signal excitation in case of S-parameter measurements is that the instantaneous voltage trajectory will cross several of these grid boxes. This is illustrated by Figure 1, where the time domain waveform of the drain-source voltage is plotted as function of the gate-source voltage time domain waveform. In this experiment, the device has been excited by a single tone signal at the gate and by a second CW signal at a different fundamental frequency at the drain. The measurements have been performed on the Non-linear Network Measurement System (2), which provides this flexibility of multi-tone two-port excitations. For the example shown in Figure 1, we notice that one large-signal measurement provides time domain measurement

data in 28 of the grid boxes with size 50 mV x 100 mV. As reported previously (3), the whole (V_1, V_2) area can be sufficiently covered with a minimum number of vectorial large-signal measurements by engineering properly the degrees of freedom of the measurement system (DC bias, input powers, input frequencies, ...). It is important to point out that the proposed procedure in this work does not require multiple trajectories through exactly the same (V_1, V_2) grid points, which is a requirement for the direct extraction method (3). Therefore, the required number of large-signal measurements can be reduced and will be significantly smaller compared to the number of S-parameter measurements needed to generate a look-up table model over this region.
For the example of an amplifier IC, we performed several vectorial large-signal measurements at various input powers and at fundamental frequencies covering the amplifier's bandwidth. The amplifier's optimal operation fixes the DC bias condition.

The next step consists in determining the level of the device's dynamics, which corresponds to the orders of voltage and current time derivatives, that have to be taken into account in Equations (1) and (2). This can be accomplished by the so-called "embedding" technique, based on the "false nearest neighbour" principle (6). This consists in unfolding the characteristics of the dependent variables (I_1, I_2) as a function of increasing number of independent variables (V_1, V_2, $\dot{V}_1$, $\dot{V}_2$, ...) until a single-valued function is obtained. The results of applying this technique to the studied HEMT and amplifier IC are displayed in Tables 1 and 2. The first column represents the dimensionality of the state space. The numbers in the second and third columns are, respectively for I_1 and I_2, the normalised number of data points that have "false" neighbours, which is an indication to check whether a single-valued function can be obtained for that dimensionality of the state space. The last column lists the state variables that have been taken into account for this calculation. When performing measurements at fundamental frequencies up to 5 GHz, we found that it is necessary to include state variables up to $\ddot{V}_1$ for I_1 and I_2 in case of the HEMT and up to $\dot{V}_1$ for I_1 and $\dot{V}_2$ for I_2 in case of the amplifier IC.

Finally, the functional relationships f_1 and f_2 of Equations (1) and (2) are determined by fitting the measured time domain data of the terminal currents to the time domain data of the independent variables, determined in the preceding step. In this work, we used polynomials to describe f_1 and f_2, but this can be replaced by other types of fitting functions.

MODELLING RESULTS

We implemented the obtained model in the Agilent ADS microwave circuit simulator by means of a symbolically defined device. An important validation of the model is to test it under limiting conditions, such as in DC or small-signal operation, because this kind of data has not been used in the modelling process. Figure 2 shows that the dynamical HEMT model predicts well the static behaviour. Next, Figures 3 and 4 present, respectively for the HEMT and for the amplifier IC, the good agreement between large-signal simulation results and NNMS measurements. We noticed that the lower-dimensional behavioural model for this amplifier IC simulates at least 30 % faster than the corresponding circuit model consisting of several models for each of the subcomponents. The obtained behavioural models are accurate as long as the instantaneous currents and voltages remain well within the operation region covered by the large-signal measurements or time-domain simulation results used in the optimisation process.

CONCLUSIONS

We presented for the first time a procedure to determine a black-box time-domain dynamical model directly from vectorial large-signal measurements and/or simulations. Advantages are that this method is not restricted to weakly non-linear behaviour and that less measurements are needed compared to the direct extraction based methods. Moreover, this method is not only applicable to microwave transistors, but also to more complicated ICs, because no physical preknowledge is required.

ACKNOWLEDGEMENTS

D. Schreurs is supported by the Fund for Scientific Research-Flanders as a post-doctoral fellow. This work has been performed in the framework of a visiting scientistship of D. Schreurs at the Agilent Technologies Microwave Technology Center.

REFERENCES

(1) F. van Raay and G. Kompa, "A new on-wafer large-signal waveform measurement system with 40 GHz harmonic bandwidth", 1992, *IEEE MTT-S Int. Microwave Symp. Digest*, pp. 1435–1438.
(2) J. Verspecht *et al.*, "Accurate On Wafer Measurement Of Phase And Amplitude Of The Spectral Components Of Incident And Scattered Voltage Waves At The Signal Ports Of A Nonlinear Microwave Device", 1995, *IEEE MTT-S Int. Microwave Symp. Digest*, pp. 1029–1032.
(3) D. Schreurs, "Overview of non-linear device modelling methods based on vectorial large-signal measurements", 1999, *Proc. European Gallium Arsenide and related III-V compounds Application Symp.*, pp. 381–386.
(4) M. Curras-Francos *et al.*, "Direct extraction of nonlinear FET I-V functions from time domain large signal measurements", 1998, *Electronics Letters*, pp. 1993–1994.
(5) J. Verspecht *et al.*, "System Level Simulation Benefits from Frequency Domain Behavioral Models of Mixers and Amplifiers", 1999, *Proc. European Microwave Conference*, pp. 29–32.
(6) M. Kennel *et al.*, "Determining embedding dimension for phase-space reconstruction using a geometrical construction", 1992, *Physical Review A*, Vol. 45, No. 6, pp. 3403–3411.

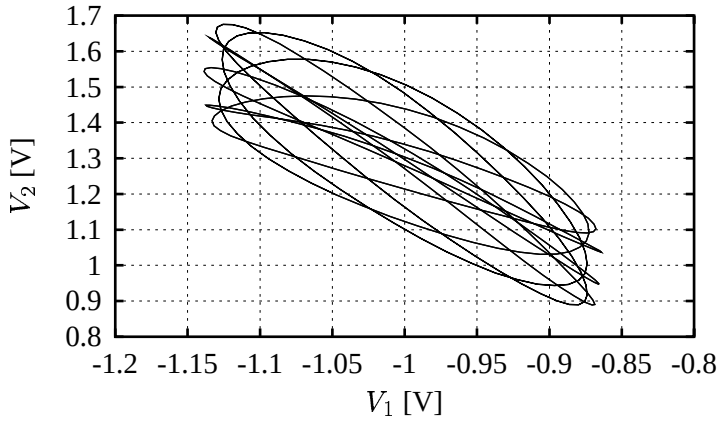

Figure 1: Example coverage of the (V_1, V_2) plane by a *single* vectorial large-signal measurement under two-tone excitation.

dimension	fnn I_1	fnn I_2	state variables
3	0.492	0.4179	$(I_1 \mid\mid I_2)$ + V_1, V_2
4	0.2504	0.2494	$(I_1 \mid\mid I_2)$ + V_1, V_2, $\dot{V}_1$
5	0.1202	0.2369	$(I_1 \mid\mid I_2)$ + V_1, V_2, $\dot{V}_1$, $\dot{V}_2$
6	0.05125	0.199	$(I_1 \mid\mid I_2)$ + V_1, V_2, $\dot{V}_1$, $\dot{V}_2$, $\ddot{V}_1$
7	0.205	0.3816	$(I_1 \mid\mid I_2)$ + V_1, V_2, $\dot{V}_1$, $\dot{V}_2$, $\ddot{V}_1$, $\ddot{V}_2$

Table 1: Normalised number of false nearest neighbours (fnn) for I_1 and I_2 of a HEMT as function of the state variables taken into consideration.

dimension	fnn I_1	fnn I_2	state variables
3	0.3449	0.3638	$(I_1 \mid\mid I_2)$ + V_1, V_2
4	0.09477	0.1444	$(I_1 \mid\mid I_2)$ + V_1, V_2, $\dot{V}_1$
5	0.1534	0.09590	$(I_1 \mid\mid I_2)$ + V_1, V_2, $\dot{V}_1$, $\dot{V}_2$
6	0.1103	0.1429	$(I_1 \mid\mid I_2)$ + V_1, V_2, $\dot{V}_1$, $\dot{V}_2$, $\ddot{V}_1$
7	0.05538	0.05206	$(I_1 \mid\mid I_2)$ + V_1, V_2, $\dot{V}_1$, $\dot{V}_2$, $\ddot{V}_1$, $\ddot{V}_2$

Table 2: Normalised number of false nearest neighbours (fnn) for I_1 and I_2 of an amplifier IC as function of the state variables taken into consideration.

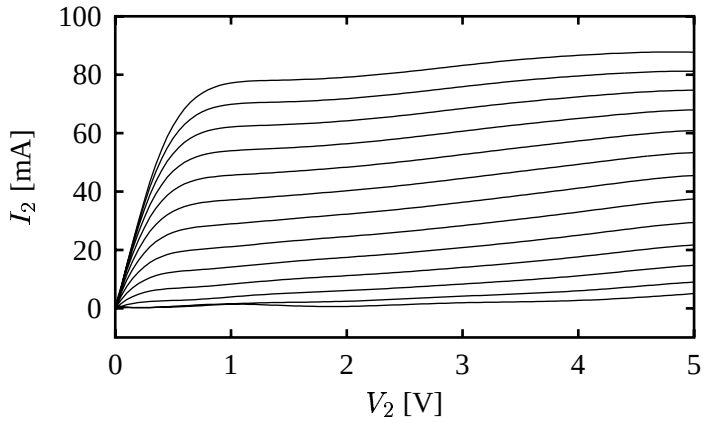

Figure 2: DC simulation of the dynamically modelled I_2 of a HEMT as function of V_2 with V_1 ranging between -1.2 V and 0 V.

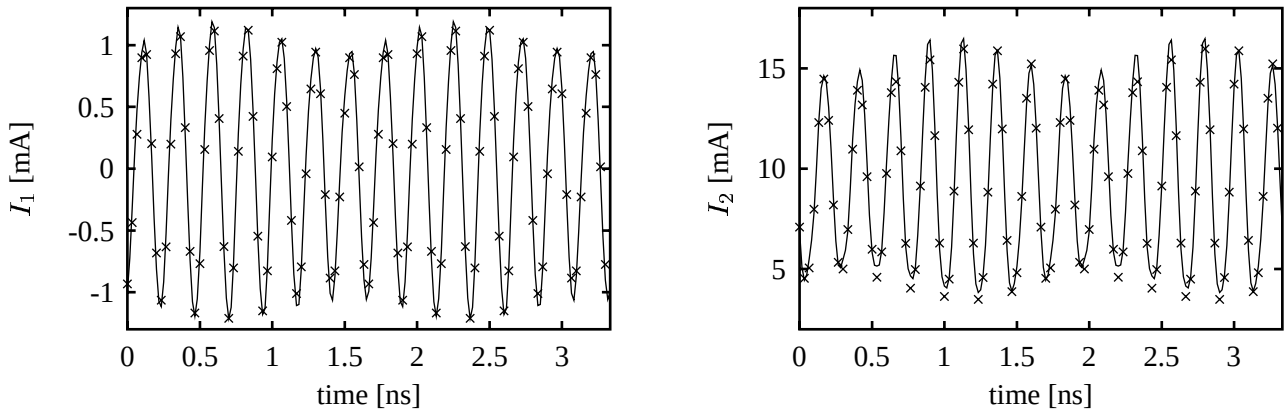

Figure 3: Comparison of the measured (x) and modelled (_) $I_1(t)$ (left) and $I_2(t)$ (right) of a HEMT under two-tone excitation.

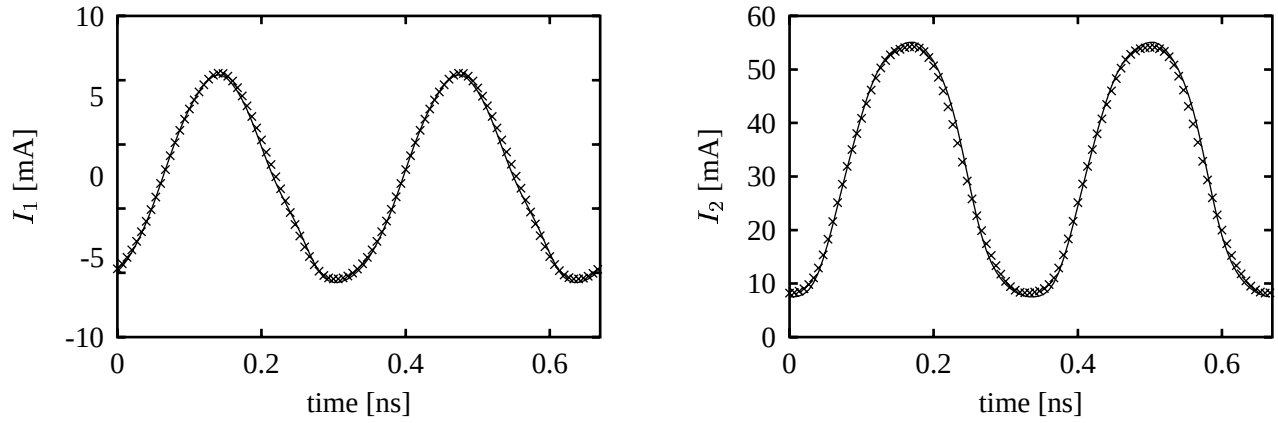

Figure 4: Comparison of the measured (x) and modelled (_) $I_1(t)$ (left) and $I_2(t)$ (right) of an amplifier IC at 3 GHz.